AD-A238 393

CONTRACTOR REPORT BRL-CR-665

BRL

THE DEVELOPMENT OF A FIBER-OPTIC READOUT PRESSURE TRANSDUCER

JOSEPH H. HARITONIDIS

JUNE 1991

U.S. ARMY LABORATORY COMMAND

BALLISTIC RESEARCH LABORATORY
ABERDEEN PROVING GROUND, MARYLAND

NOTICES

UNCLASSIFIED

REPORT DOCUMENTATION PAGE

Form Approved
OMB No. 0704-0188

1. AGENCY USE ONLY *(Leave blank)*	2. REPORT DATE	3. REPORT TYPE AND DATES COVERED
	June 1991	Final, Jun 90 - Jan 91.

4. TITLE AND SUBTITLE

The Development of a Fiber-Optic Readout Pressure Transducer

5. FUNDING NUMBERS

PR: 1L162618AH80

DAAL03-86-D-0001

6. AUTHOR(S)

Joseph H. Haritonidis

7. PERFORMING ORGANIZATION NAME(S) AND ADDRESS(ES)

320D Bolz Hall
2036 Neil Avenue
Columbus, OH 43210

8. PERFORMING ORGANIZATION REPORT NUMBER

9. SPONSORING/MONITORING AGENCY NAME(S) AND ADDRESS(ES)

US Army Ballistic Research Laboratory
ATTN: SLCBR-DD-T
Aberdeen Proving Ground, MD 21005-5066

10. SPONSORING/MONITORING AGENCY REPORT NUMBER

BRL-CR-665

11. SUPPLEMENTARY NOTES

The Contracting Officer's Representative for this report is Bradford S. Davis, Launch and Flight Division, U.S. Army Ballistic Research Laboratory, Aberdeen Proving Ground, MD 21005-5066.

12a. DISTRIBUTION/AVAILABILITY STATEMENT

Approved for public release; distribution is unlimited.

12b. DISTRIBUTION CODE

13. ABSTRACT *(Maximum 200 words)*

An all-optical pressure measurement system has been developed that uses a highly reflective diaphragm as the sensing element for a pressure transducer. This type of pressure transducer offers improved sensitivity, free from electrical and magnetic disturbances. Laser light is reflected off of the fiber's end and from the diaphragm. The reflections travel back into the same fiber and are combined interferometrically to create interference fringes. These fringes shift proportionally to the diaphragm's deflection. The return signal is sent to a photodetector and analyzed for pressure variations.

14. SUBJECT TERMS

Pressure measurement, fiber optics, lasers, interferometry

15. NUMBER OF PAGES

16

16. PRICE CODE

17. SECURITY CLASSIFICATION OF REPORT	18. SECURITY CLASSIFICATION OF THIS PAGE	19. SECURITY CLASSIFICATION OF ABSTRACT	20. LIMITATION OF ABSTRACT
UNCLASSIFIED	UNCLASSIFIED	UNCLASSIFIED	SAR

NSN 7540-01-280-5500

UNCLASSIFIED

Standard Form 298 (Rev 2-89)
Prescribed by ANSI Std Z39-18
298-102

INTENTIONALLY LEFT BLANK.

Table of Contents

INTENTIONALLY LEFT BLANK.

List of Figures

Page

INTENTIONALLY LEFT BLANK.

I. Introduction

Many applications exist in the ballistic research and development area that require an accurate pressure measurement determination. An all-optical pressure measurement system offers the potential of being free from both electrical and magnetic disturbances. A Scientific Services Contract (STAS) was awarded to assist the Ballistic Research Laboratory (BRL), Launch and Flight Division (LFD), Free Flight Aerodynamics Branch (FFAB), with the design and assembly of a prototype fiber-optic pressure transducer, similar to one built at MIT for pressure measurements in turbulent boundary layers[1,2]. This transducer is covered by patents #4926696 and #4942767. Additionally, the STAS was intended to bring LFD, FFAB up-to-date on current fiber-optic/laser technology and assess the usefulness of a fiber optic measurement scheme in a ballistic research setting.

In the following report, background material is presented on pressure transducers, the particulars of fiber-optic transducers, and the design and construction of the prototype transducer built at BRL. Design specifications for a high-pressure transducer are also presented in the Appendix.

II. Technical Background

1. Diaphragm Pressure Transducers

The most common type of pressure transducer is of the diaphragm type as shown in Fig. 1

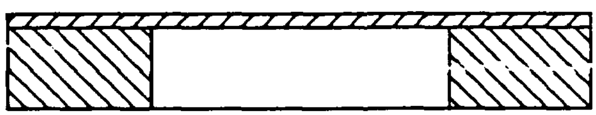

Figure 1. Schematic of a diaphragm pressure transducer.

A diaphragm, attached to a substrate, is exposed to a pressure difference, Δp, under the action of which it deflects up or down. For small deflections, typically of the order of 1% maximum of its lateral extent or less than 1/3 of the diaphragm thickness, the deflection is proportional to the applied pressure difference.[3] The measurement of pressure is therefore reduced to measuring the diaphragm displacement.

It will be useful to define a spatial or geometric sensitivity for any given type of transducer in connection with the primary change of the transducer when exposed to a pressure difference. In the case of diaphragm transducers, the primary change is the displacement of the diaphragm from its equilibrium position. The spatial sensitivity will be the ratio of the maximum displacement of the diaphragm, say at its middle, to some reference length. For example, in the case of a capacitive-type transducer, the reference length will be the distance between the two capacitor plates.

The two most common methods of measuring displacement are a) by measuring the change in capacitance of a capacitor formed by the diaphragm itself and a reference plate positioned below it, and b) using strain gauges mounted on the diaphragm itself.

The spatial sensitivity of the capacitive-type transducer will depend on the position of the reference plate given a fixed displacement of the diaphragm. The closer the two plates are, the higher the spatial sensitivity, and thus the larger the change in capacitance. This is desirable since it is easier to detect large relative changes than smaller ones. However, the closer the plates are, the more the diaphragm will be obstructed in rapid motion in trying to displace the fluid between the capacitor plates.

The use of strain gauges, which are often deposited on the diaphragm, are susceptible to errors due to temperature effects, even at low temperatures. In addition, very high quality electronics are necessary since the change in resistance of the strain gauges is very small. In this case, the spatial sensitivity is approximately equal to the ratio of the diaphragm displacement to the radius of the diaphragm, which is indeed very small. For the typical maximum displacement of 1% of the diameter, it translates to a strain of about 2%, or a resistance change of about 4% if the strain gauges have a typical gage factor of 2.

2. Interferometric Transducers

A much better spatial sensitivity can be obtained when using interferometry. The diaphragm displacement is measured through the interference of coherent light reflected off the diaphragm and a reference surface. The particular transducer described in this report uses the end of a single mode fiber, the optical flat, as the reference surface (see Fig. 2).

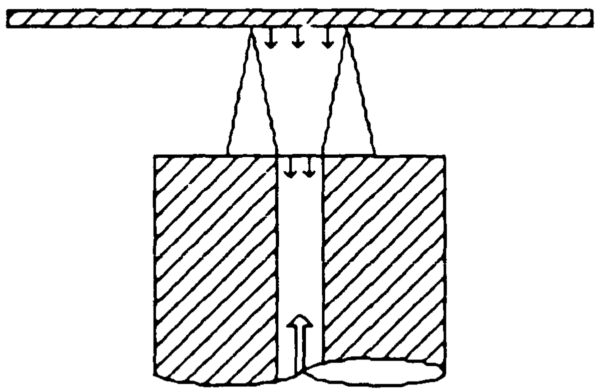

Figure 2. Optical-fiber interferometry.

In this case, the spatial sensitivity is the ratio of the diaphragm displacement to that of the wavelength of light used. It becomes immediately apparent that the sensitivity may now be too much rather than too little. For example, a diaphragm displacement of 1% of the diaphragm diameter is equal to 10μm for a diaphragm 1 mm in diameter. Using a He-Ne laser, with a wavelength of 0.633μm, the spatial sensitivity is about 1600% rather than a few percent. Using this type of sensitivity, an interferometric transducer has been built as described in References 4 and 5. This type of sensitivity, however, makes use of fairly intricate digital electronics, required to count fringes, compared to very simple analog electronics for an interferometric transducer with a maximum spatial sensitivity less than 100%.

The intensity, I, of the two interfering waves reflected off the diaphragm and the end of the fiber varies almost sinusoidally with distance, S, of the diaphragm displacement, as shown in Fig. 3.

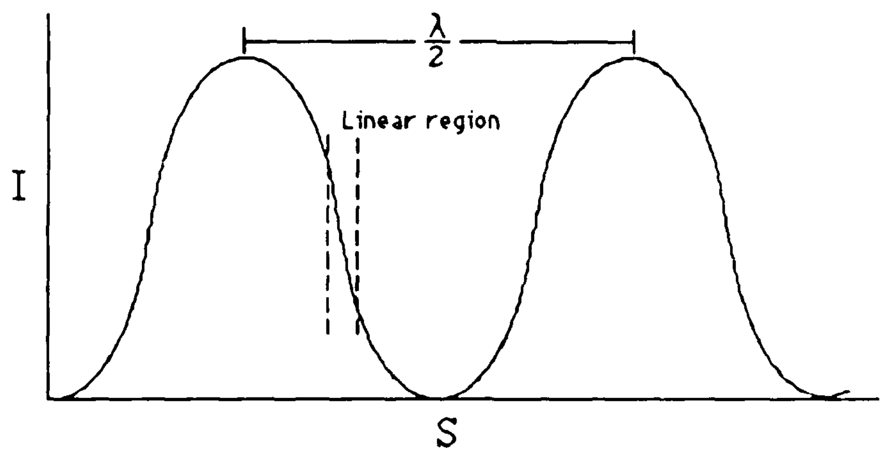

Figure 3. Intensity vs. diaphragm displacement.

If the initial displacement is such that the intensity is at half its maximum value with no pressure difference present, then applied pressure differences will cause the intensity to vary, initially, linearly with applied pressure. If the displacement of the diaphragm remains between the short vertical lines shown in Fig. 3, then a linear variation of intensity with displacement will be obtained.

III. System Description

1. System Components

The overall system setup is shown in Fig. 4. A 1mW, frequency and amplitude stabilized, He-Ne laser (Spectra-Physics™, model 117A-1) was used as the coherent light source. The light beam was then coupled into a single mode fiber using a Newport™ F-916 coupler with a 20x objective lens. The laser and the coupler were mounted on a Newport™ XSD-13 breadboard. The single mode fiber (4μm core diameter, 125μm cladding) is one of four pigtails of an Aster™ 50/50 fiber coupler (model SMC-01-50-2-A-1-S). Half of the light leaving the fiber coupler is lost without reflections at the terminator which consists of a 4-40 screw around which the fiber is wound about 15 turns. The other half of the light is directed to the sensor.

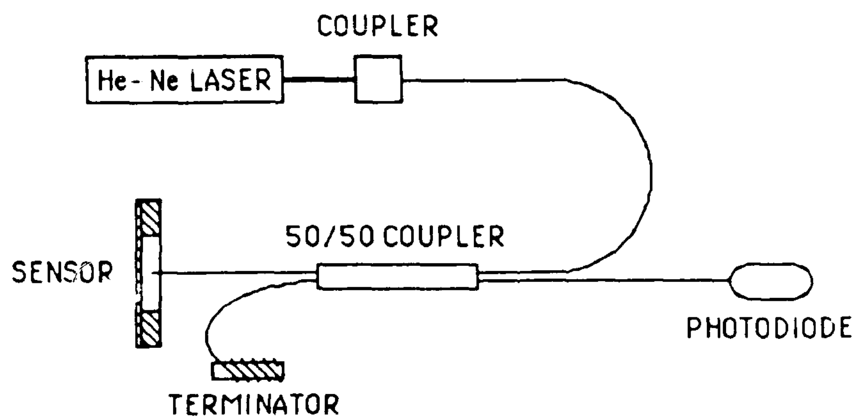

Figure 4. Overall setup.

About 4% of that light is reflected off the end of the fiber, opposite the diaphragm, and is directed back towards the fiber coupler. Of the light emerging from the end of the fiber, about 4% is also captured by the fiber after reflection off the polished diaphragm. While 96% of the light leaves the fiber end, a much smaller percentage comes back due to the fact that the light spreads out conically on its way to the diaphragm and back. By adjusting the initial separation distance, S, between the fiber end and the back of the diaphragm, the captured light is of the same intensity as that reflected off the end of the fiber, thus enabling complete destructive interference when the two reflected waves are 180 degrees out of phase. It is this

geometric arrangement that produces the graph of intensity vs. separation distance shown in Fig. 3.

After reaching the fiber coupler, half of the reflected light travels back towards the laser and the other half towards the photodiode (EG&G JUDSON™, model HAD-1100A).

2. Pressure Sensor

A pressure sensor was designed for measuring pressures of the order of 104Pa (1.5psi). The diaphragm was made from a common, single edge, razor blade with a thickness of 0.23mm (0.009in). The diaphragm was mounted on an aluminum base as shown in Fig. 5.

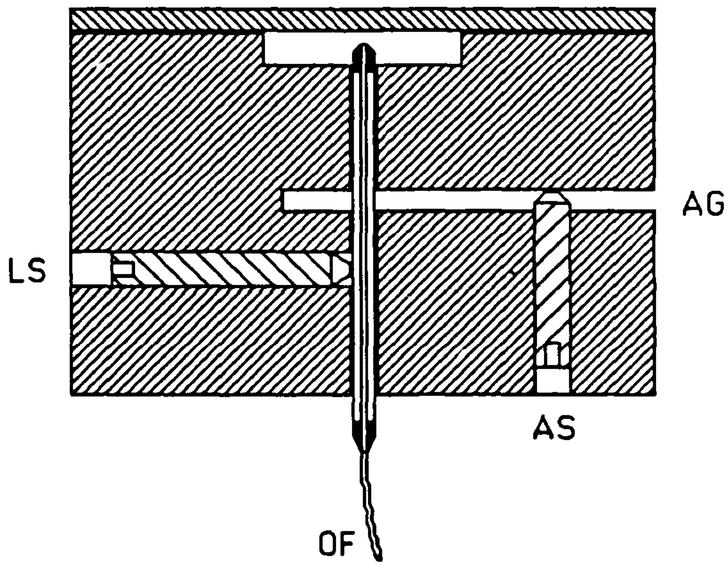

Figure 5. Pressure sensor schematic.

The active diaphragm diameter is approximately 8mm. This dimension was dictated by the requirement that under the maximum applied pressure, i.e. 1.5psi, the diaphragm at hand should deflect no more than about 10% of λ or 0.06μm. This small deflection ensures that the diaphragm displacement is linear with applied pressure to very high accuracy. The following equation was used to calculate the diaphragm diameter, valid for small deflections for a circular diaphragm[5]:

$$\delta = \frac{3r^4(1-\nu^4)}{16Et^3}\Delta p$$

where,

δ	= diaphragm center displacement
r	= diaphragm radius
v	= Poisson's ratio
Δp	= applied pressure difference
E	= Young's modulus
t	= diaphragm thickness

It is evident that care should be taken in the calculations since the displacement is very sensitive to the actual diaphragm thickness and radius.

The last 2cm of fiber (OF) were secured in 1.5mm O.D. hypodermic tube with epoxy glue. The tube was held in place in the aluminum base with a lock screw (LS). Manual adjustment of the tube position, and hence the fiber-end distance from the diaphragm, was initially done to make sure that the two reflected waves were of the same intensity for optimum performance, as discussed earlier. Once this was accomplished, fine adjustments were made with the adjusting screw (AS) so that the intensity of the observed interfering waves was half the maximum value. By the previous adjustment, the minimum intensity (destructive interference) was zero. The purpose of the adjusting gap, which is approximately 1.5mm wide, is to allow for infinitesimal movements of the fiber end relative to the reflective surface. This was accomplished by fixing the fiber via the locking screw to the lower part of the aluminum base and ever so slightly separating the upper part through the use of the adjusting screw. This method proved to be very effective since the fiber end position has to be adjusted to within a fraction of a micron with respect to the diaphragm.

3. Photodiode Circuit

The photodiode circuit is shown in Fig. 6. A pair of 12V lantern batteries are used to power both the photodiode amplifier and the second stage external amplifier. Batteries were used for the convenience of low noise; however, it would be preferable to use a good quality power supply to ensure voltage stability. A high pass filter, with a low frequency cutoff of 16Hz, is used to subtract the relatively large intensity (half of the maximum intensity) to isolate the fluctuations in the linear region. Thus, only the deviations from the equilibrium position are amplified at the second stage.

If slower pressure fluctuations are to be measured, then a high pass filter with a lower cutoff frequency can be easily implemented. The present circuit has the advantage of being very simple compared to circuits required for any other pressure transducer of comparable sensitivity.

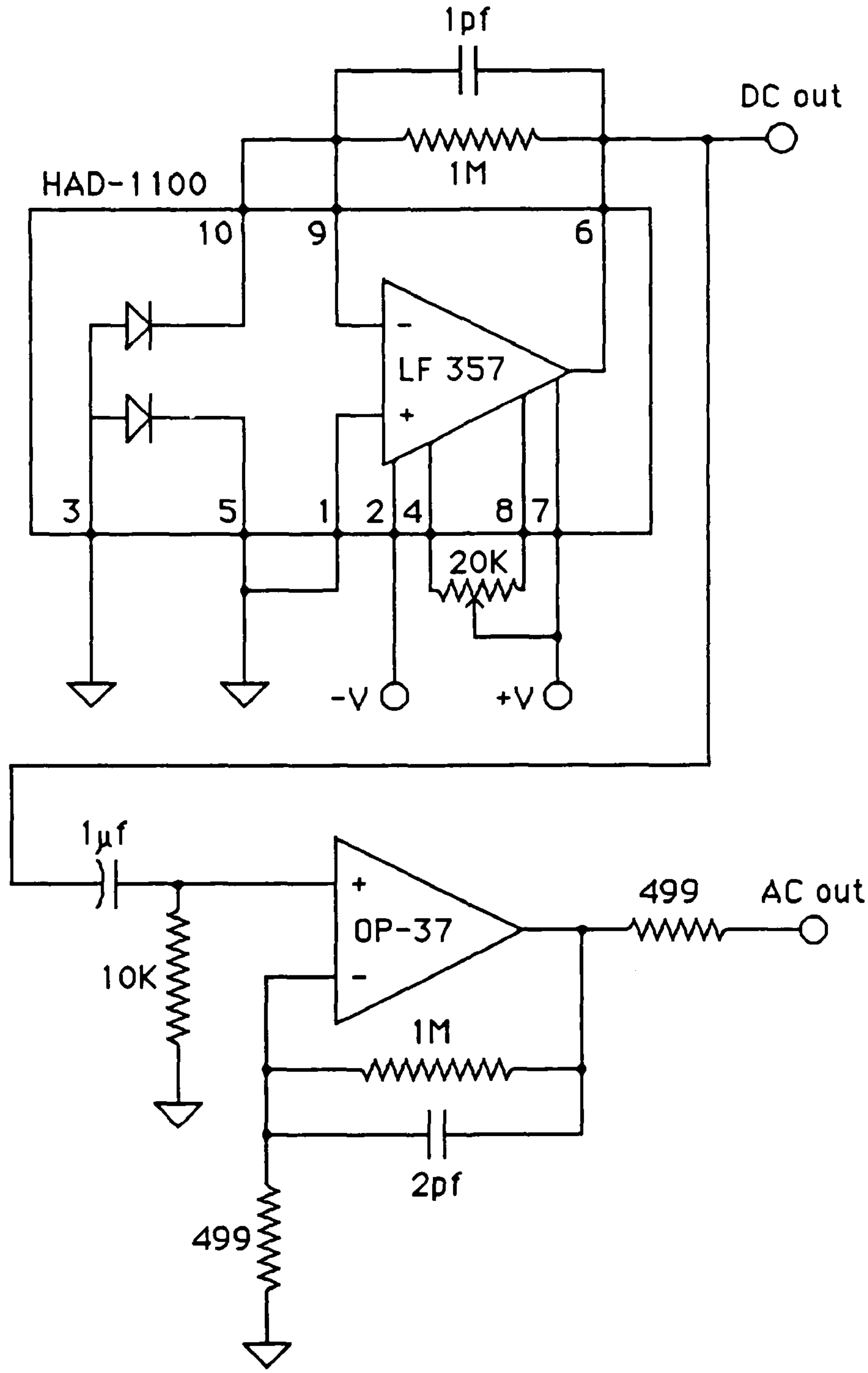

Figure 6. Photodiode circuit.

4. Performance

The performance of the overall system was within expected bounds. The intensity variations, as observed on an oscilloscope when the diaphragm was blown upon, were clearly visible and somewhat larger than expected since the pressures generated were well below 1.5psi. Due to time constraints, the system was not fine-tuned for optimum performance, a task to be undertaken at a later date by BRL.

A source of noise, manifested as intensity fluctuations and identified in References 1 and 2, was also observed in this case, and is due to motion of the fiber (jiggling). It is not clear at this point by what mechanism this comes about.

IV. Conclusions

An interferometric pressure measuring system was built, similar to the one developed in References 1 and 2. A new type of pressure sensor was developed in this case with an improved adjustment method for setting the operating point. Improvements in the overall setup will be achieved when a better understanding of the noise source is obtained, as discussed above.

The system described in the Appendix holds promise for measuring the very large pressures generated in a gun breech using the same interferometric arrangement described here, but with a different sensing mechanism. Future plans also include replacing the He-Ne laser with a laser diode and miniaturizing the electronic circuit with microchips and surface mount technology.

Appendix

The measurement of gun tube breech and chamber pressure are currently made with conventional piezo-electric transducers. These electronic sensors are inherently susceptible to electromagnetic (EM) interference. The basic principles of operation of the optical transducer make it suitable for measuring a wide range of gun tube pressure values without EM signal degradation. However, since gun breech and chamber pressures approach 10^5psi, even diaphragms made of the optimum materials begin to suffer from plastic deformation thus rendering them unsuitable for pressure measurement. This appendix describes a variation of the system presented in the main report that appears to hold promise for measuring very large gun pressures with excellent spatial and temporal response.

The basic arrangement of the new transducer is shown in Figure A1.

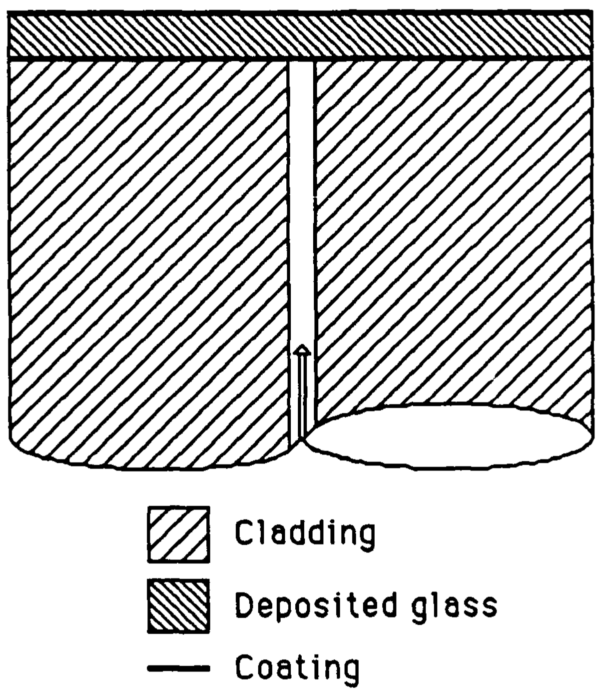

Figure A1. Schematic of the high pressure sensor.

Three layers of material are deposited directly on the end of the fiber. The first layer is a reflective coating, the second a relatively thick layer of glass and the third another reflective coating. Interfering waves now come from reflections off the end of the fiber and the top part of the glass layer. The reflective coatings are necessary to achieve equal reflected intensities back into the fiber.

The sensing mechanism is now through the compression of the glass layer. However, in this case the interferometer's intensity vs. thickness (or distance between the two reflective coatings) of the glass layer looks more like a picket fence, as shown in Figure A2

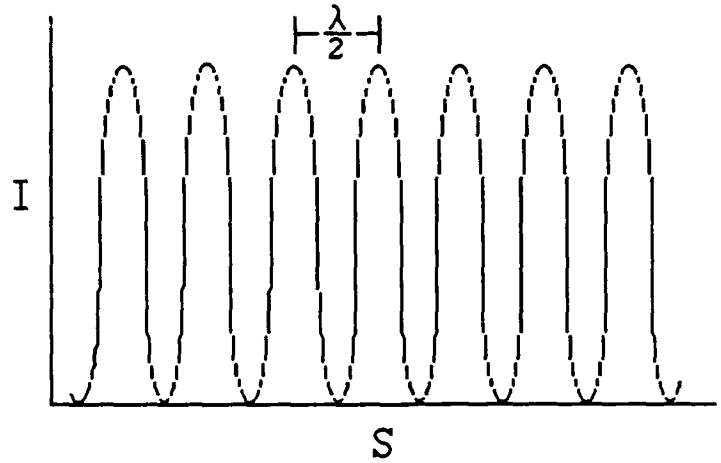

Figure A2. Intensity vs. glass layer thickness.

As in the previous case, the distance between peaks in the interference pattern is still $\lambda/2$. The configuration causes the slope to much steeper about the half intensity level. The advantage is that the sensitivity is much greater, but a disadvantage may be that it is much more difficult to fabricate the various layers to the desired thickness, in particular the middle sensing layer.

The thickness of the glass, sensing layer, is determined by two requirements. The first is that the thickness should be such that under the expected maximum strain, the thickness change will be about 5% of the wavelength of light used, resulting in a path length change of 10%. The second requirement is that the thickness should be rounded off to an integral number of half-wavelengths plus an eighth so that with no applied pressure the intensity level is at half its maximum value. In addition, it should be remembered that the wavelength of light will be altered in the glass layer due to the index of refraction, n.

The strain $\varepsilon = \sigma/E$, where σ is the applied stress and E is Young's modulus for the particular glass deposited. Therefore, the change in glass thickness will be $\Delta s = \varepsilon S$, where S is the thickness of the glass layer. We now set $\Delta s = 0.05\lambda/n$ so that $S = \Delta s/\varepsilon = 0.05\lambda E/(n\sigma)$. Using $n = 1.5$ for the index of refraction of glass, $\lambda = 0.633\mu m$, $E = 5 \times 10^6$ psi and $\sigma = 10^5$ psi, we find $S \approx 1.055\mu m$. We now set $S = m(\lambda/2n) \pm \lambda/8n$ which gives $m = 5$. Ideally, $m = 4.75$ which implies that our sensitivity for a planned 0.05λ change in S will be 5% less, an acceptable change. Conversely, if we do allow a

0.05λ change in thickness for S, then we can increase the pressure range by 5%. In either case, the design thickness will be $S_d = 1.108\mu m$.

Finally, some mention should be made in regards to the temperature sensitivity of this arrangement. Glass has a typical coefficient of thermal expansion of $9 \times 10^{-6}/°K$. If we require our measurement to be accurate to within 1%, then we can tolerate long term temperature changes of about ± 21°K. Under normal circumstances, this is very acceptable. If, however, the sensor is exposed to very high temperatures, then the question is how large a temperature change can be tolerated for how long, so that the measurement error is within prescribed limits.

The problem to be solved here is the classical heat conduction problem in a semi-infinite slab when an impulsive temperature change takes place at its surface. The solution to this problem is readily obtained as $F(\eta) = (T-T_1)/(T_2-T_1) = erf(\eta)$, where T is the temperature in the slab, T_1 is the surface temperature before the imposed temperature jump, T_2 is the imposed temperature, erf is the error integral and $\eta = s/2(\alpha t)^{1/2}$,where α is the thermal diffusivity of the slab material, and s and t are the distance in the slab and time respectively where and when T is evaluated. For small values of $F(\eta)$, we may approximate the solution, to very good accuracy, as $F(\eta) = 1.13\eta$.

We now assume that the we can tolerate a maximum error of 5% in pressure measurement with a gun tube temperature jump of 2000°K. According to our discussion earlier, a 5% error due to temperature translates to an average temperature in the glass layer of 5x(21°K) = 105°K. We therefore take half this temperature to be the temperature at the bottom of the glass layer and seek the time it will take for this to occur. With $\alpha = 0.005 cm^2/s$ and $s = 1.1\mu m$, we find that the time it takes for this to occur is about 1ms. It is seen that this is a borderline case. However, as the time of heat penetration is proportional to the square of the glass layer, one way to improve the situation is to deposit an additional insulating layer on top of the top reflective layer. Thus, an additional 3µm thick layer will increase the useful operating time of the sensor to 9ms.

INTENTIONALLY LEFT BLANK.

References

1. "Optical Micropressure Transducer", 1990. Haritonidis, J. H., Mehregany, M., Senturia, S. D. & Warkentin, D., Patent # 4926696.

2. "Pressure Transducer Apparatus", 1990. Haritonidis, J. H., Mehregany, M., Senturia, S. D. & Warkentin, D., Patent # 4942767.

3. "An In-Process Twin-Interferometer Distortion Monitor for Tungsten Sputtered Films", 1988. Goldsberry, J. E., M.S. Thesis, Department of Electrical Engineering & Computer Science, M.I.T.

4. "A Twin-Interferometer Fiber-Optic Readout for Diaphragm Pressure Transducers", 1989. Young, A. M-H., M.S. Thesis, Department of Electrical Engineering & Computer Science, M.I.T.

5. Measurement Systems, 1975. Doebelin, E. O., McGraw-Hill, New York.

INTENTIONALLY LEFT BLANK.

No. of Copies	Organization
2	Administrator Defense Technical Info Center ATTN: DTIC-DDA Cameron Station Alexandria, VA 22304-6145
1	Commander U.S. Army Materiel Command ATTN: AMCDRA-ST 5001 Eisenhower Avenue Alexandria, VA 22333-0001
1	Commander U.S. Army Laboratory Command ATTN: AMSLC-DL 2800 Powder Mill Road Adelphi, MD 20783-1145
2	Commander U.S. Army Armament Research, Development, and Engineering Center ATTN: SMCAR-IMI-I Picatinny Arsenal, NJ 07806-5000
2	Commander U.S. Army Armament Research, Development, and Engineering Center ATTN: SMCAR-TDC Picatinny Arsenal, NJ 07806-5000
1	Director Benet Weapons Laboratory U.S. Army Armament Research, Development, and Engineering Center ATTN: SMCAR-CCB-TL Watervliet, NY 12189-4050
nclass. only) 1	Commander U.S. Army Armament, Munitions and Chemical Command ATTN: AMSMC-IMF-L Rock Island, IL 61299-5000
1	Director U.S. Army Aviation Research and Technology Activity ATTN: SAVRT-R (Library) M/S 219-3 Ames Research Center Moffett Field, CA 94035-1000

No. of Copies	Organization
1	Commander U.S. Army Missile Command ATTN: AMSMI-RD-CS-R (DOC) Redstone Arsenal, AL 35898-5010
1	Commander U.S. Army Tank-Automotive Command ATTN: ASQNC-TAC-DIT (Technical Information Center) Warren, MI 48397-5000
1	Director U.S. Army TRADOC Analysis Command ATTN: ATRC-WSR White Sands Missile Range, NM 88002-5502
1	Commandant U.S. Army Field Artillery School ATTN: ATSF-CSI Ft. Sill, OK 73503-5000
(Class. only) 1	Commandant U.S. Army Infantry School ATTN: ATSH-CD (Security Mgr.) Fort Benning, GA 31905-5660
(Unclass. only) 1	Commandant U.S. Army Infantry School ATTN: ATSH-CD-CSO-OR Fort Benning, GA 31905-5660
1	Air Force Armament Laboratory ATTN: WL/MNOI Eglin AFB, FL 32542-5000

Aberdeen Proving Ground

No. of Copies	Organization
2	Dir, USAMSAA ATTN: AMXSY-D AMXSY-MP, H. Cohen
1	Cdr, USATECOM ATTN: AMSTE-TD
3	Cdr, CRDEC, AMCCOM ATTN: SMCCR-RSP-A SMCCR-MU SMCCR-MSI
1	Dir, VLAMO ATTN: AMSLC-VL-D
10	Dir, BRL ATTN: SLCBR-DD-T

INTENTIONALLY LEFT BLANK.

USER EVALUATION SHEET/CHANGE OF ADDRESS

This laboratory undertakes a continuing effort to improve the quality of the reports it publishes. Your comments/answers below will aid us in our efforts.

1. Does this report satisfy a need? (Comment on purpose, related project, or other area of interest for which the report will be used.) ______

2. How, specifically, is the report being used? (Information source, design data, procedure, source of ideas, etc.) ______

3. Has the information in this report led to any quantitative savings as far as man-hours or dollars saved, operating costs avoided, or efficiencies achieved, etc? If so, please elaborate. ______

4. General Comments. What do you think should be changed to improve future reports? (Indicate changes to organization, technical content, format, etc.) ______

BRL Report Number BRL-CR-665 Division Symbol ______

Check here if desire to be removed from distribution list. ____

Check here for address change. ____

Current address: Organization ______
Address ______

DEPARTMENT OF THE ARMY
Director
U.S. Army Ballistic Research Laboratory
ATTN: SLCBR-DD-T
Aberdeen Proving Ground, MD 21005-5066

OFFICIAL BUSINESS

NO POSTAGE NECESSARY IF MAILED IN THE UNITED STATES

BUSINESS REPLY MAIL
FIRST CLASS PERMIT No 0001, APG, MD

Postage will be paid by addressee

Director
U.S. Army Ballistic Research Laboratory
ATTN: SLCBR-DD-T
Aberdeen Proving Ground, MD 21005-5066